that hERα expressed in *Drosophila* was able to activate the ERE reporter gene and respond to hERα agonists and antagonists in the same manner that had been observed in mammalian cells and tissues (McDonnell *et al.* 1995; Metzger *et al.* 1995; Watanabe *et al.* 2001). As hERα transgenic flies appear to be normal in terms of growth and reproduction, without any overt abnormalities, it seems that human steroid hormone receptors do not significantly interfere with endogenous signalling pathways. It can also be inferred that exogenous human steroid receptors do not compete with endogenous NRs at the fly NR-responsive elements in target gene promoters (Talbot *et al.* 1993; McKenna & O'Malley 2002). Therefore, our results provided evidence that transgenic *Drosophila* expressing hERα represent a potent and functionally relevant system in which to evaluate NR synthetic ligands and to genetically identify and characterize novel NR co-regulators.

### Pivotal role of Ser$^{118}$ in the hERα ligand-induced transactivation function *in vivo*

Both N-terminal AF-1 and C-terminal AF-2 domains contribute to the hERα ligand-induced transactivation function, with each AF-1 and AF-2 activity dependent on promoter-context and cell type (Kumar *et al.* 1987; Tora *et al.* 1989). The balance between hERα AF-1 and AF-2 is thought to be responsible, at least in part, for the tissue-specific action of selective oestrogen receptor modulators (SERMs) such as tamoxifen (Berry *et al.* 1990; McDonnell *et al.* 1995; Metzger *et al.* 1995; Brzozowski *et al.* 1997; Shiau *et al.* 1998). In particular, the activity of hERα AF-1 is believed to support the oestrogenic actions of SERMs (Endoh *et al.* 1999; Watanabe *et al.* 2001), leading to beneficial actions of SERMs in certain tissues such as the improved bone properties in oestrogen-related pathophysiological states (Shang & Brown 2002). Therefore, while the physiological and pharmacological significance of hERα AF-1 activity has been well addressed, the molecular basis underlying AF-1 function remains to be elucidated in terms of identifying the relevant specific co-regulators and co-regulator complexes (Endoh *et al.* 1999; Watanabe *et al.* 2001). The core activation region of hERα AF-1 has been mapped to the middle of the A/B domain (Kobayashi *et al.* 2000), and a number of *in vitro* studies have indicated that the Ser$^{118}$ residue in this core region appears to play a crucial role and can be phosphorylated by several kinases in response to extracellular signals (Kato *et al.* 1995; Chen *et al.* 2000). Nevertheless, the impact of Ser$^{118}$ phosphorylation *in vivo* remains obscure because of lack of studies involving intact animals. The present findings provide for the first time *in vivo* evidence for the significance of Ser$^{118}$ phosphorylation in the transcriptional activity of the AF-1 domain alone and in the transactivation function of hERα as a whole receptor.

### *In vivo* potentiation of hERα AF-1 through Cdk7-mediated phosphorylation of Ser$^{118}$

It has been shown that hERα Ser$^{118}$ can be phosphorylated by several kinases (Ali *et al.* 1993; Le *et al.* 1994; Kato *et al.* 1995; Chen *et al.* 2000). Cdk7 has been chosen for the present study as mutant flies with inactive Cdk7 appear to suffer more general defects in gene regulation (Austin & Biggin 1996). We have shown that Cdk7 phosphorylates hERα Ser$^{118}$ *in vivo* and that this phosphorylation enhanced hERα AF-1 activity in normal flies. It has been shown recently that, besides direct receptor phosphorylation, MAPKs are also able to potentiate function of some hERα co-activators, including AIB1, through phosphorylation of the cofactor protein (Font de Mora & Brown 2000). This suggests an additional mechanism for downstream cross-talk between different signalling pathways. Our transgenic *Drosophila* provides an experimental system in which to further study whether MAPKs activated by growth factors or stress-induced signalling pathways can also modulate hERα activity.

### Ser$^{118}$ phosphorylation-dependent and -independent co-activators for hERα

The S118A hERα mutant retained ligand responsiveness, albeit with reduced transactivation. Transactivation in the S118A hERα mutant has nevertheless been significantly enhanced by over-expression of TAI, *Drosophila* AIB1 homologue. Therefore, it appears that hERα activity is modulated *in vivo* by both phosphorylation-dependent and phosphorylation-independent co-activators. However, the timing of the recruitment of these co-activators, presumably within co-factor complexes associated with the AF-1 domain, remains unclear. p68/p72 have been identified as hERα AF-1-specific co-activators that physically associate with the hERα AF-1 domain (Endoh *et al.* 1999; Watanabe *et al.* 2001). Significantly, this interaction was clearly not dependent on Ser$^{118}$ phosphorylation. It is not clear, however, whether recruitment of most of known hERα co-activators is dependent on phosphorylation status of the receptor. In this respect, the transgenic *Drosophila* lines that express hERα and its mutants represent a powerful tool for genetic screening of phosphorylation-dependent and -independent co-factors.

## Experimental procedures

### Transfection and luciferase activity

hERα mutants and dCdk7 expression vectors were constructed using the pCaSpeR vector for expression in Schneider cells. hERα mutants and dCdk7 expression plasmids (0.05 μg) were co-transfected with 0.2 μg actin-GAL4 plasmid and 0.5 μg ERE-tk-luc plasmid, along with 10 ng pRL-CMV-luc plasmid as an internal control. Three hours after transfection, the ligands $10^{-8}$ M 17β-oestradiol (Sigma, St Louis, MO), $10^{-8}$ M tamoxifen (Sigma) or $10^{-8}$ M ICI 182.780 (Tocris Cookson, Ballwin, MO) were added. After 20 h, dual luciferase assays were performed as previously described (Yanagisawa *et al.* 2002).

### Generation of transgenic flies and *Drosophila* stocks

For germ-line transformation into *Drosophila*, cDNA encoding hERα mutants and GFP reporter under control of ERE-containing promoter were inserted into pCaSpeR. Transgenic constructs together with pπ25.7wc transposase were microinjected into $w^{1118}$ embryos using a micromanipulator (Leica). Several independent transformant lines were established. To express hERα in *Drosophila* eyes, transgenic lines were crossed with a *GMR-GAL4* line that expressed GAL4 in the retina under the control of the glass multimer reporter. The *tai*$^{EY08809}$, *UAS-tai*, *Df(1)J8254*-Pw$^{-}$[*snf*$^{-}$, *dld*$^{-}$] and *cdk7*$^{x}$ mutants were obtained from the Bloomington *Drosophila* Stock Center. The *nej*$^{3}$ and *GMR-GAL4* line were the generous gifts of Drs S. Ishii and Y. Hiromi, respectively.

### Histology

Eye imaginal discs from third instar larvae were dissected and fixed for 20 min in 4% formaldehyde at 25 °C. Eye discs were incubated with primary antibodies HC-20 (Santa Cruz Biotechnology, Santa Cruz, CA) or B10 that recognize the C- and N-terminal regions of hERα, respectively. Cy5-conjugated Affinity Pure donkey anti-rabbit or anti-mouse IgG (Jackson Immuno-Research, West Grove, PA) were used as secondary antibodies for immunofluorescence staining. hERα and GFP expression were detected using a Zeiss Confocal Laser Scanning System 510.

### Western blotting

To confirm hERα and GFP expression in *Drosophila*, cell lysates from the heads of adult flies of third instar larvae were separated by 15% SDS–PAGE and detected with anti-ERα antibodies (HC-20 or B10) and anti-GFP antibody (Santa Cruz Biotechnology), and expression levels measured using Adobe Photoshop software facility. Fold-activation of hERα in *Drosophila* was shown as GFP expression signal intensity normalizing with hERα expression signal intensity.

### *In vitro* phosphorylation

293T cells were transfected with FLAG tagged dCdk7 expression plasmid, lysed in lysis buffer, and immunoprecipitated with anti-FLAG affinity gel (Sigma). hCdk7 was obtained from 293T cells by immunoprecipitation with Cdk7 (N-19) antibody (Santa Cruz Biotechnology). dCdk7 or hCdk7 (9 μg) were incubated for 20 min at 30 °C with purified bacterially produced 10 μg of GST-fused hERα (amino acids 56–180 of hERα) and its mutants or GST-fused human retinoic acid receptor α1 (hRARα1) (Rochette-Egly *et al.* 1997), in 50 mM Tris-HCl, 0.5 mM EDTA, 25 mM $MgCl_2$, 1 mM DTT, 20 μM ATP, 0.01 μCi [γ-$^{32}$P]ATP and 10% glycerol. Phosphorylation of substrates was analysed by 12% sodium dodecyl sulphate–polyacrylamide gel electrophoresis (SDS–PAGE) and autoradiography. Expression of GST-hERα mutants and GST-hRARα1 were detected by CBB staining.

## Acknowledgements

We thank H. Tanimoto, K. Suneizumi, M. Sato, A. Watanabe, Y. Takei, D. Umetsu, I. Takada, F. Ohtake, H. Endoh, T. Furutani, Y. Masuhiro, A. Nishida, Y. Mezaki, R. Fujiki, A. Maki, E. Suzuki, Y. Zhao and K. Yamagata for helpful discussions and H. Higuchi for support. We also thank Dr S. Ishii for the *nej*$^{3}$ fly, Dr Y. Hiromi for the *GMR-GAL4* fly and Dr P. Chambon for hERα expression vectors and anti-hERα antibody (B10). This work was supported by a grant-in-aid for priority areas from the Ministry of Education, Culture, Sports, Science and Technology of Japan (K.T. and S.K.) and Basic Research Activities for Innovative Biosciences (BRAIN) (S.K.).

## References

Akimaru, H., Chen, Y., Dai, P., *et al.* (1997) *Drosophila* CBP is a co-activator of cubitus interruptus in hedgehog signalling. *Nature* **386**, 735–738.

Ali, S., Metzger, D., Bornert, J.M. & Chambon, P. (1993) Modulation of transcriptional activation by ligand-dependent phosphorylation of the human oestrogen receptor A/B region. *EMBO J.* **12**, 1153–1160.

Austin, R.J. & Biggin, M.D. (1996) Purification of the *Drosophila* RNA polymerase II general transcription factors. *Proc. Natl. Acad. Sci. USA* **93**, 5788–5792.

Bai, J., Uehara, Y. & Montell, D.J. (2000) Regulation of invasive cell behavior by taiman, a *Drosophila* protein related to AIB1, a steroid receptor coactivator amplified in breast cancer. *Cell* **103**, 1047–1058.

Baker, K.D., Shewchuk, L.M., Kozlova, T., *et al.* (2003) The *Drosophila* orphan nuclear receptor DHR38 mediates an atypical ecdysteroid signaling pathway. *Cell* **113**, 731–742.

Belandia, B. & Parker, M.G. (2003) Nuclear receptors: a rendezvous for chromatin remodeling factors. *Cell* **114**, 277–280.

Berry, M., Metzger, D. & Chambon, P. (1990) Role of the two activating domains of the oestrogen receptor in the cell-type and promoter-context dependent agonistic activity of the anti-oestrogen 4-hydroxytamoxifen. *EMBO J.* **9**, 2811–2818.

Brand, A.H. & Perrimon, N. (1993) Targeted gene expression as a means of altering cell fates and generating dominant phenotypes. *Development* **118**, 401–415.

Brzozowski, A.M., Pike, A.C., Dauter, Z., *et al.* (1997) Molecular basis of agonism and antagonism in the oestrogen receptor. *Nature* **389**, 753–758.

Chen, D., Riedl, T., Washbrook, E., *et al.* (2000) Activation of estrogen receptor alpha by S118 phosphorylation involves a ligand-dependent interaction with TFIIH and participation of CDK7. *Mol. Cell* **6**, 127–137.

Chen, H., Lin, R.J., Schiltz, R.L., *et al.* (1997) Nuclear receptor coactivator ACTR is a novel histone acetyltransferase and forms a multimeric activation complex with P/CAF and CBP/p300. *Cell* **90**, 569–580.

Ciana, P., Raviscioni, M., Mussi, P., *et al.* (2003) *In vivo* imaging of transcriptionally active estrogen receptors. *Nat. Med.* **9**, 82–86.

Couse, J.F. & Korach, K.S. (1999) Estrogen receptor null mice: what have we learned and where will they lead us? *Endocr. Rev.* **20**, 358–417.

Egly, J.M. (2001) The 14th Datta Lecture. TFIIH: from transcription to clinic. *FEBS Lett.* **498**, 124–128.

Endoh, H., Maruyama, K., Masuhiro, Y., *et al.* (1999) Purification and identification of p68 RNA helicase acting as a transcriptional coactivator specific for the activation function 1 of human estrogen receptor α. *Mol. Cell Biol.* **19**, 5363–5372.

Fondell, J.D., Ge, H. & Roeder, R.G. (1996) Ligand induction of a transcriptionally active thyroid hormone receptor coactivator complex. *Proc. Natl. Acad. Sci. USA* **93**, 8329–8333.

Font de Mora, J. & Brown, M. (2000) AIB1 is a conduit for kinase-mediated growth factor signaling to the estrogen receptor. *Mol. Cell Biol.* **20**, 5041–5047.

Freedman, L.P. (1999) Increasing the complexity of coactivation in nuclear receptor signaling. *Cell* **97**, 5–8.

Frit, P., Bergmann, E. & Egly, J.M. (1999) Transcription factor IIH: a key player in the cellular response to DNA damage. *Biochimie* **81**, 27–38.

Glass, C.K. & Rosenfeld, M.G. (2000) The coregulator exchange in transcriptional functions of nuclear receptors. *Genes Dev.* **14**, 121–141.

Heery, D.M., Kalkhoven, E., Hoare, S. & Parker, M.G. (1997) A signature motif in transcriptional co-activators mediates binding to nuclear receptors. *Nature* **387**, 733–736.

Kamei, Y., Xu, L., Heinzel, T., *et al.* (1996) A CBP integrator complex mediates transcriptional activation and AP-1 inhibition by nuclear receptors. *Cell* **85**, 403–414.

Kato, S., Endoh, H., Masuhiro, Y., *et al.* (1995) Activation of the estrogen receptor through phosphorylation by mitogen-activated protein kinase. *Science* **270**, 1491–1494.

Kitagawa, H., Fujiki, R., Yoshimura, K., *et al.* (2003) The chromatin-remodeling complex WINAC targets a nuclear receptor to promoters and is impaired in Williams syndrome. *Cell* **113**, 905–917.

Kobayashi, Y., Kitamoto, T., Masuhiro, Y., *et al.* (2000) p300 mediates functional synergism between AF-1 and AF-2 of estrogen receptor α and β by interacting directly with the N-terminal A/B domains. *J. Biol. Chem.* **275**, 15645–15651.

Kumar, V., Green, S., Stack, G., *et al.* (1987) Functional domains of the human estrogen receptor. *Cell* **51**, 941–951.

Larochelle, S., Chen, J., Knights, R., *et al.* (2001) T-loop phosphorylation stabilizes the CDK7-cyclin H-MAT1 complex *in vivo* and regulates its CTD kinase activity. *EMBO J.* **20**, 3749–3759.

Le, G.P., Montano, M.M., Schodin, D.J. & Katzenellenbogen, B.S. (1994) Phosphorylation of the human estrogen receptor. Identification of hormone-regulated sites and examination of their influence on transcriptional activity. *J. Biol. Chem.* **269**, 4458–4466.

McDonnell, D.P., Clemm, D.L., Hermann, T., Goldman, M.E. & Pike, J.W. (1995) Analysis of estrogen receptor function *in vitro* reveals three distinct classes of antiestrogens. *Mol. Endocrinol.* **9**, 659–669.

McKenna, N.J. & O'Malley, B.W. (2002) Combinatorial control of gene expression by nuclear receptors and coregulators. *Cell* **108**, 465–474.

Metivier, R., Penot, G., Hubner, M.R., *et al.* (2003) Estrogen receptor-α directs ordered, cyclical, and combinatorial recruitment of cofactors on a natural target promoter. *Cell* **115**, 751–763.

Metzger, D., Berry, M., Ali, S. & Chambon, P. (1995) Effect of antagonists on DNA binding properties of the human estrogen receptor *in vitro* and *in vivo*. *Mol. Endocrinol.* **9**, 579–591.

Moses, K. & Rubin, G.M. (1991) Glass encodes a site-specific DNA-binding protein that is regulated in response to positional signals in the developing *Drosophila* eye. *Genes Dev.* **5**, 583–593.

Naar, A.M., Beaurang, P.A., Zhou, S., *et al.* (1999) Composite co-activator ARC mediates chromatin-directed transcriptional activation. *Nature* **398**, 828–832.

Onate, S.A., Tsai, S.Y., Tsai, M.J. & O'Malley, B.W. (1995) Sequence and characterization of a coactivator for the steroid hormone receptor superfamily. *Science* **270**, 1354–1357.

Rachez, C., Lemon, B.D., Suldan, Z., *et al.* (1999) Ligand-dependent transcription activation by nuclear receptors requires the DRIP complex. *Nature* **398**, 824–828.

Rochette-Egly, C., Adam, S., Rossignol, M., Egly, J.M. & Chambon, P. (1997) Stimulation of RAR α activation function AF-1 through binding to the general transcription factor TFIIH and phosphorylation by CDK7. *Cell* **90**, 97–107.

Shang, Y. & Brown, M. (2002) Molecular determinants for the tissue specificity of SERMs. *Science* **295**, 2465–2468.

Shiau, A.K., Barstad, D., Loria, P.M., *et al.* (1998) The structural basis of estrogen receptor/coactivator recognition and the antagonism of this interaction by tamoxifen. *Cell* **95**, 927–937.

Spencer, T.E., Jenster, G., Burcin, M.M., *et al.* (1997) Steroid receptor coactivator-1 is a histone acetyltransferase. *Nature* **389**, 194–198.

Takeyama, K., Ito, S., Yamamoto, A., *et al.* (2002) Androgen-dependent neurodegeneration by polyglutamine-expanded human androgen receptor in *Drosophila*. *Neuron* **35**, 855–864.

Talbot, W.S., Swyryd, E.A. & Hogness, D.S. (1993) *Drosophila* tissues with different metamorphic responses to ecdysone express different ecdysone receptor isoforms. *Cell* **73**, 1323–1337.

Tora, L., White, J., Brou, C., *et al.* (1989) The human estrogen receptor has two independent nonacidic transcriptional activation functions. *Cell* **59**, 477–487.

Watanabe, M., Yanagisawa, J., Kitagawa, H., *et al.* (2001) A subfamily of RNA-binding DEAD-box proteins acts as an estrogen receptor α coactivator through the N-terminal activation domain (AF-1) with an RNA coactivator, SRA. *EMBO J.* **20**, 1341–1352.

Yanagisawa, J., Kitagawa, H., Yanagida, M., *et al.* (2002) Nuclear receptor function requires a TFTC-type histone acetyl transferase complex. *Mol. Cell* **9**, 553–562.

Yuan, C.X., Ito, M., Fondell, J.D., Fu, Z.Y. & Roeder, R.G. (1998) The TRAP220 component of a thyroid hormone receptor-associated protein (TRAP) coactivator complex interacts directly with nuclear receptors in a ligand-dependent fashion. *Proc. Natl. Acad. Sci. USA* **95**, 7939–7944.

*Received*: 27 May 2004
*Accepted*: 12 July 2004

Molecular Human Reproduction vol.6 no.5 pp. 443–447, 2000

# Distribution of steroidogenic enzymes involved in androgen synthesis in polycystic ovaries: an immunohistochemical study

**Eugenie M.Kaaijk[1,2,4], Hironobu Sasano[3], Takashi Suzuki[3], Johan F.Beek[2] and Fulco van der Veen[1]**

[1]Center for Reproductive Medicine, Department of Obstetrics and Gynaecology, Academic Medical Center, Amsterdam, [2]Laser Center, Academic Medical Center, Amsterdam, The Netherlands, and [3]Department of Pathology, Tohoku University School of Medicine, Aoba-ku, Sendai 980-8595, Japan

[4]To whom correspondence should be addressed at: Center for Reproductive Medicine, Department of Obstetrics and Gynaecology, Academic Medical Center, PO Box 22660, 1105 AZ Amsterdam, The Netherlands

**To find an explanation for the possible working mechanism of laparoscopic ovarian electrocautery for the treatment of anovulation in polycystic ovarian syndrome (PCOS), we evaluated the distribution of steroidogenic enzymes involved in the synthesis of ovarian androgens in surgical pathology specimens of entire polycystic ovaries. A total of 13 formalin-fixed and paraffin-embedded samples of the ovaries of patients with clinically proven PCOS were immunostained with specific antibodies against cholesterol side-chain-cleavage enzyme (P450scc), 3β-hydroxysteroid dehydrogenase (3β-HSD), 17α-hydroxylase (P450c17) and adrenal 4-binding protein (Ad4BP), a transcription factor of steroidogenic enzymes. Follicular theca cells of all ovaries demonstrated marked immunoreactivity for Ad4BP, P450scc, 3β-HSD and P450c17. Granulosa cells of seven ovaries expressed Ad4BP, while granulosa cells of three ovaries also showed P450scc. In the granulosa cells of all ovaries, 3β-HSD and P450c17 immunoreactivity was not observed. In the stroma, luteinized cells of most ovaries demonstrated Ad4BP, P450scc, 3β-HSD and P450c17 immunoreactivity, but at a much lower level compared with the follicular theca cells. Non-luteinized stromal cells sporadically demonstrated Ad4BP, P450scc, 3β-HSD and P450c17 immunoreactivity. The stromal steroidogenic cells were mainly located in the ovarian cortex, except for some hilus steroidogenic cells. These data demonstrate that in polycystic ovaries, androgens are mainly produced in the follicular theca cells and to some extent in luteinized stromal cells. This suggests that the working mechanism of laparoscopic electrocautery of the ovary is primarily explained through the reduction of ovarian hyperandrogenism by coagulation of follicular theca cells and concomitant stroma.**

*Key words:* 17α hydroxylase/ovarian stroma/ovarian surgery/polycystic ovary/side chain cleavage enzyme

## Introduction

Laparoscopic electrocautery and laparoscopic laser surgery can restore ovulation in clomiphene-resistant patients with polycystic ovary syndrome (PCOS). These treatments act on the ovarian surface, thereby creating a varying number of holes in the ovarian capsule. This results in destruction of subcapsular follicles and/or subcapsular stroma. Postoperative endocrine alterations observed in most studies after laparoscopic ovarian surgery include a decrease in LH as well as a decrease in serum androstenedione and testosterone concentrations, preceding the return of ovulatory cycles (Kaaijk *et al.*, 1994). The factor responsible for restoration of ovulation after laparoscopic ovarian surgery in PCOS is unknown but the endocrine alterations suggest that reduction of ovarian hyperandrogenism caused by destruction of androgen-producing tissue plays an important role in restoring ovulation (Cohen, 1996). In this view it is important to know which compartment of the polycystic ovary is responsible for androgen production. We have found four studies which measured androgen production in polycystic ovaries by in-vitro culture experiments (Warren and Salhanick, 1961; Biggs and Thomas, 1981; Mori *et al.*, 1982; Haney *et al.*, 1986). The limitations of these studies are that they are small, lack uniformity, and measure androgen production in only small pieces of polycystic ovarian tissue obtained by wedge resection. Two of these four studies measured androgen production in the ovarian cortex and in the medulla and found that androgens were mainly produced in the ovarian cortex (Warren and Salhanick, 1961; Biggs and Thomas, 1981). The other two studies measured androgen production in follicular theca cells and cortical stroma, and found that the follicular theca cells are much more involved in androgen production than cortical stroma (Mori *et al.*, 1982; Haney *et al.*, 1986). Two studies determined androgen production in the ovarian cortex of polycystic ovaries by immunohistochemical techniques (Tamura *et al.*, 1993; Takayama *et al.*, 1996). These studies concluded that androgens were mainly derived from the follicular theca cells. On the other hand another author (Speroff *et al.*, 1994) states that stromal theca cells, derived from follicular atresia, secrete significant amounts of androstenedione and testosterone, although the author does not reference this statement. The

available evidence at this moment therefore suggests that follicular theca cells are the main sites of androgen production in PCOS but the contribution of the ovarian stroma and medulla in androgen production is still not well established.

In this study, we therefore used entire polycystic ovaries to evaluate the contribution of the ovarian stroma, medulla and the follicular theca cells to androgen production by immunolocalization of steroidogenic enzymes involved in androgen production. In addition, the presence of adrenal 4-binding protein (Ad4BP), a universal transcription factor of steroidogenic enzymes, which has been almost exclusively detected in steroid producing cells, was studied (Sasano *et al.*, 1995; Takayama *et al.*, 1995).

## Materials and methods

### *Ovaries*

Ovaries were obtained from 13 patients who had undergone unilateral oophorectomy 14–18 years previously as treatment of clomiphene-resistant anovulation ($n$ = 7) or oligomenorrhoea in combination with severe hirsutism and cycle irregularities ($n$ = 6). The ages of the patients were 22–36 years at the time of unilateral oophorectomy. All patients had oligomenorrhoea, elevated testosterone concentrations (>4 nmol/l) and LH/FSH ratios >3.

The ovaries were fixed in 10% formalin and embedded in paraffin 14–18 years previously. Light microscopic examination of all 13 haematoxylin and eosin-stained ovaries showed the presence of a thickened ovarian capsule with multiple subcapsular cysts and a dense hyperplastic ovarian stroma (Figure 1).

### *Immunohistochemistry*

Surgical pathology specimens of the ovaries were cut into 3 μm thick sections and mounted on poly-L-lysine-coated glass slides. The primary antibodies used for this study were all polyclonal antibodies produced in rabbits. The optimal dilutions and the sources including their characteristics have been previously described (Takayama *et al.*, 1996).

Immunostaining was performed as previously described (Suzuki *et al.*, 1994). Briefly, after routine deparaffinization, sections were placed in 0.3% $H_2O_2$-methyl alcohol for 30 min to block endogenous peroxidase activity. Slides for Ad4BP immunostaining were placed in citric acid buffer (2 mmol/l citric acid, 9 mmol/l trisodium citrate dihydrate, pH 6.0), heated in a microwave oven (model NE-A40; Matsushita, Tokyo, Japan) for 15 min (500 W) for antigen retrieval, and subsequently allowed to cool down for ~2 h at room temperature. Sections were treated for 30 min at room temperature with 10% normal goat serum.

Immunohistochemical studies were performed using the streptavidin–biotin–peroxidase method with a Histofine kit (Nichirei Co Ltd, Tokyo, Japan). Sections were incubated with primary antibodies for 18 h at 4°C. They were then incubated for 30 min at room temperature with biotinylated anti-rabbit immunoglobulin (Ig)G, washed with 0.01 mol/l phosphate-buffered saline (PBS) and incubated with peroxidase-conjugated streptavidin under the same conditions as described above. The reaction product was subsequently detected by immersion in a solution containing 0.05 mol/l Tris–HCl, pH 7.6, 0.66 mol/l 3.3′-diaminobenzidine (DAB) and 2 mol/l $H_2O_2$. A 1% methyl green staining solution was employed for counterstaining the nuclei. As negative controls, 0.01 mol/l PBS, normal rabbit IgG and unrelated antibodies, including adrenocorticotrophic, were used instead of the primary antibodies.

The immunoreactivity of the steroidogenic enzymes and Ad4BP was independently evaluated and graded as follows by two of the authors (H.S. and T.S.): − = cells no immunoreactivity; + = number of positive cells <25% of the total number of cells; ++ = number of positive cells in 25–50% of the total number of cells; +++ = number of positive cells in >50% of the total number of cells. Discordant ovaries were re-evaluated simultaneously by the same authors, using double-headed light microscopy (BH-2, Olympus Co Ltd, Tokyo, Japan). Follicular cells were classified into theca cells and granulosa cells. Stromal cells were classified into luteinized and non-luteinized cells. Luteinized stromal cells were histologically defined as cells associated with abundant clear or eosinophilic cytoplasm. Non-luteinized stromal cells were defined as the stromal cells not presenting abundant clear or eosinophilic cytoplasm.

## Results

Immunoreactivity of Ad4BP, P450scc, 3β-HSD and P450c17 appeared brown as a result of DAB colorimetric reaction. Immunoreactivity of steroidogenic enzymes was detected in the cytoplasm, while that of Ad4BP was detected in the nucleus.

Immunoreactivity for these enzymes and grading of positive follicular theca cells (TC), granulosa cells (GC), stromal luteinized cells (LC) and non-luteinized cells (NL) are summarized in Table I.

In all ovaries, the follicular theca cells demonstrated Ad4BP (Figure 2), P450scc (Figure 3), 3β-HSD (Figure 4) and P450c17 (Figure 5). In seven ovaries, the granulosa cells were positive for Ad4BP, and in three ovaries these cells were positive for P450scc. These three ovaries were also immunopositive for Ad4BP. 3β-HSD and P450c17 immunoreactivity was not detected in any of the granulosa cells of the follicles examined.

In the stroma, luteinized cells of 11 ovaries demonstrated Ad4BP, P450scc, and P450c17 immunoreactivity, while 12 ovaries demonstrated 3β-HSD immunoreactivity. In non-luteinized stromal cells, Ad4BP nuclear immunoreactivity was present in eight ovaries. P450scc immunoreactivity was present in the non-luteinized stromal cells of six ovaries which also presented Ad4BP nuclear immunoreactivity. 3β-HSD and P450c17 were present in four and three ovaries respectively. The number of luteinized cells and non-luteinized cells positive for Ad4BP, 3β-HSD and P450c17 was lower compared with that of positive theca cells.

Apart from some immunopositive hilus cells (Figure 6), the majority of the stromal cells showing immunoreactivity for the steroidogenic enzymes and Ad4BP were distributed in the outer cortical stroma of the ovary (Figures 7 and 8).

## Discussion

The results of this study, the first that determined steroidogenic enzymes involved in androgen synthesis in entire polycystic ovaries, show that follicular theca cells, as well as luteinized stromal cells demonstrate Ad4BP, P450scc, 3β-HSD and P450c17 immunoreactivity, and that therefore these cells are capable of producing androgens. Furthermore, some non-luteinized stromal cells of some ovaries showed immunoreactivity for these enzymes. However, the total number of immunopositive luteinized and non-luteinized stromal cells is much

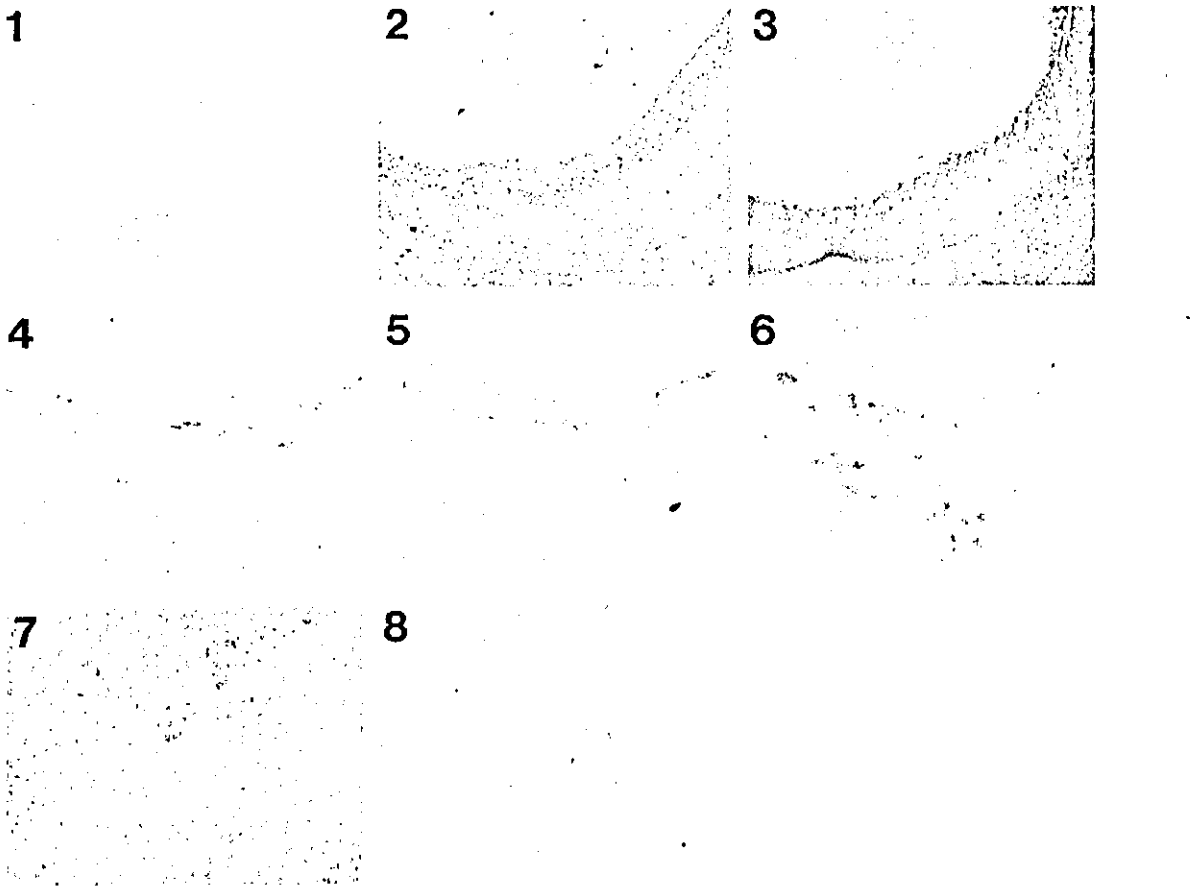


**Figure 1.** Gross section of a haematoxylin and eosin-stained polycystic ovary (magnification ×1.6).

**Figure 2.** Immunoreactivity of adrenal 4-binding protein (Ad4BP) in the theca cells of the polycystic ovary shown in Figure 1 (magnification ×50).

**Figure 3.** Immunoreactivity of cholesterol side-chain-cleavage enzyme (P450scc) in the theca cells of the polycystic ovary shown in Figure 1 (magnification ×50).

**Figure 4.** Immunoreactivity of 3β-hydroxysteroid dehydrogenase (3β-HSD) in the theca cells of the polycystic ovary shown in Figure 1 (magnification ×66).

**Figure 5.** Immunoreactivity of 17α-hydroxylase (P450c17) in the theca cells of the polycystic ovary shown in Figure 1 (magnification ×66).

**Figure 6.** Immunoreactivity of 3β-hydroxysteroid dehydrogenase (3β-HSD) in the hilar region of the polycystic ovary shown in Figure 1 (magnification ×66).

**Figure 7.** Immunoreactivity of 3β-hydroxysteroid dehydrogenase (3β-HSD) in the cortical stroma of the polycystic ovary shown in Figure 1 (magnification ×66).

**Figure 8.** Immunoreactivity of 17α-hydroxylase (P450c17) in the inner stroma of the polycystic ovary shown in Figure 1 (magnification ×66).

lower than that of follicular theca cells, suggesting much less involvement of the stromal cells in androgen production compared with follicular theca cells. This finding confirms the results of previous studies (Mori *et al.*, 1982; Haney *et al.*, 1986; Tamura *et al.*, 1993; Takayama *et al.*, 1996) but is in conflict with the statement of Speroff (Speroff *et al.*, 1994). Probably, most of the stromal theca cells, derived from follicular atresia, lose their capability to produce androgens. A recent study (Kyei-Mensah *et al.*, 1998) measuring ovarian stromal volume using three dimensional ultrasound in patients

**Table I.** Immunohistochemical localization of steroidogenic enzymes in the follicles and stromal tissue

| | Ad4BP | | | | P450scc | | | | 3β-HSD | | | | P450c17 | | | |
|---|---|---|---|---|---|---|---|---|---|---|---|---|---|---|---|---|
| | Follicles | | Stroma | | Follicles | | Stroma | | Follicles | | Stroma | | Follicles | | Stroma | |
| Case | TC | GC | LC | NL | TC | GC | LC | NL | TC | GC | LC | NL | TC | GC | LC | NL |
| 1 | ++ | + | ++ | + | ++ | ++ | + | + | ++ | – | + | – | ++ | – | + | – |
| 2 | +++ | + | + | + | ++ | – | + | + | ++ | – | + | + | ++ | – | + | + |
| 3 | ++ | – | ++ | – | ++ | – | ++ | – | ++ | – | ++ | – | ++ | – | ++ | – |
| 4 | ++ | – | + | + | ++ | – | + | + | ++ | – | ++ | + | ++ | – | ++ | + |
| 5 | +++ | + | × | + | + | – | × | + | ++ | – | × | + | + | – | × | – |
| 6 | ++ | + | + | + | ++ | – | + | + | ++ | – | + | + | ++ | – | + | + |
| 7 | ++ | + | + | – | + | – | + | – | + | – | + | – | + | – | + | – |
| 8 | ++ | – | + | – | + | – | + | – | ++ | – | + | – | ++ | – | + | – |
| 9 | ++ | – | + | – | ++ | – | ++ | – | ++ | – | + | – | ++ | – | + | – |
| 10 | ++ | ++ | ++ | + | ++ | ++ | ++ | – | ++ | – | + | – | ++ | – | + | – |
| 11 | ++ | + | ++ | + | ++ | + | ++ | – | ++ | – | + | – | + | – | × | – |
| 12 | ++ | – | + | + | ++ | – | + | + | ++ | – | + | – | ++ | – | + | – |
| 13 | + | – | × | – | + | – | × | – | ++ | – | + | – | ++ | – | + | – |

Immunoreactivity was graded as follows: × = cells not present; – = negative; + = positive, <25%; ++ = 25–50% positivity; +++ = >50% positivity.
TC = thecal cells; GC = granulosa cells; LC = stromal luteinized cells; NL = non-luteinized cells.

with PCOS and comparing the findings with serum androgen concentrations, demonstrated a positive correlation between stromal volume and serum androgen concentrations. This suggests that the large size of the stromal compartment in PCOS might allow stromal androgen production to become clinically significant despite a much lower involvement of stromal cells in androgen production compared to follicular theca cells, as demonstrated in our study.

An important finding of our study is that the stromal immunopositive cells are mainly present in the outer cortex, while immunopositive cells are not present in the medulla, apart from some immunopositive hilus cells. This strongly suggests that stromal androgen production in polycystic ovaries is derived from the cyst-bearing ovarian cortex. This confirms the results of the previous studies (Warren and Salhanick, 1961; Biggs and Thomas, 1981).

Based on the results of the present study, we conclude that the follicular theca cells are the main sites of androgen production, followed by luteinized stromal cells in the cortex. These results might explain why laparoscopic surgery, which acts on the ovarian surface and subcapsular follicles, results in an immediate decrease of serum androgen concentrations. This fall in serum androgen concentrations leads to a correction of the ovarian pituitary feedback, resulting in follicular growth and ovulation. The duration of regular ovulatory cycles after ovarian surgery might depend on the volume of androgen producing tissue that is destroyed and the severity of ovarian hyperandrogenism.

The drawback of laparoscopic treatments is the risk of peri-ovarian adhesion formation associated with extensive capsular damage. Donesky and Adashi have pointed out that because of the risk of adhesion formation, attention is shifting towards methods that cauterize extensive areas of the deeper stromal areas with minimal damage to the ovarian surface (Donesky and Adashi, 1995). The results of our study suggest that destruction of deeper stromal tissue alone might not reduce androgen-producing tissue sufficiently to restore ovulation. This hypothesis is supported by our preliminary clinical experience on the use of transvaginal interstitial laser treatment of the ovaries to restore ovulation in clomiphene-resistant patients with PCOS (Kaaijk *et al.*, 1997).

In summary, we demonstrated that steroidogenic enzymes involved in androgen production in the polycystic ovary are mainly expressed in the follicular theca cells and to a lesser extent in the ovarian cortical stroma. Therefore, we suggest that the working mechanism of laparoscopic electrocautery of the ovary might be primarily explained by coagulation of follicular theca cells and concomitant stroma.

## References


Biggs, J.S.G. and Thomas, F.J. (1981) Sites of steroid production in the polycystic ovary. *Br. J. Obstet. Gynaecol.*, **88**, 42–46.

Cohen, J. (1996) Laparoscopic procedures for treatment of infertility related to polycystic ovarian syndrome. *Hum. Reprod. Update*, **2**, 337–344.

Donesky, B.W. and Adashi, E.Y. (1995) Surgically induced ovulation in the polycystic ovary syndrome: Wedge resection revisited in the age of laparoscopy. *Fertil. Steril.*, **63**, 439–463.

Haney, A.F., Maxson, W.S. and Schomberg, D.W. (1986) Compartimental ovarian steroidogenesis in polycystic ovary syndrome. *Obstet. Gynecol.*, **68**, 638–644.

Kaaijk, E.M., Beek, J.F. and van der Veen, F. (1994) Laparoscopic laser surgery of chronic hyperandrogenic anovulation. *Laser Surg. Med.*, **16**, 292–302.

Kaaijk, E.M., van der Veen, F., Beek, J.F. *et al.* (1997) Transvaginal interstitial laser treatment of the ovary for the management of chronic hyperandrogenic anovulation: First clinical experience. *Gynecol. Obstet. Invest.*, **44**, 115–119.

Kyei-Mensah, A., LinTan, S., Zaidi, J. and Jacobs, H.S. (1998) Relationship of ovarian stromal volume to serum androgen concentrations in patients with polycystic ovary syndrome. *Hum. Reprod.*, **13**, 1437–1441.

Mori, T., Fujita, Y., Nihnobu, K. *et al.* (1982) Significance of atretic follicles as the site of androgen production in polycystic ovaries. *J. Endocrinol. Invest.*, **5**, 209–214.

Takayama, K., Fukaya, T., Sasano, H. *et al.* (1996) Immunohistochemical study of steroidogenesis and cell proliferation in the polycystic ovarian syndrome. *Hum. Reprod.*, **11**, 1387–1392.

Takayama, K., Sasano, H., Fukaya, T. *et al.* (1995) Immunohistochemical localization of Ad4-binding protein with correlation to steroidogenic enzyme

expression in cycling human ovaries and sex cord stromal tumors. *J. Clin. Endocrinol. Metab.*, **80**, 2815–2821.

Tamura, T., Kitawaki, J., Yamamoto, T. *et al.* (1993) Immunohistochemical localization of 17α-hydroxylase/C17-20 lyase and aromatase cytochrome P-450 in polycystic human ovaries. *J. Endocrinol.*, **139**, 503–509.

Sasano, H., Shizawa, S., Suzuki, T. *et al.* (1995) Ad4BP in the human adrenal cortex and its disorders. *J. Clin. Endocrinol. Metab.*, **80**, 2378–2380.

Speroff, L., Glass, R.H. and Kase, N. (eds) (1994) *Clinical Gynecologic Endocrinology and Infertility.* Williams and Wilkins, Baltimore, USA, 465 pp.

Suzuki, T., Sasano, H., Kimura, N. *et al.* (1994) Immunohistochemical distribution of progesterone, androgen and oestrogen receptors in the human ovary during the menstrual cycle: Relationship to expression of steroidogenic enzymes. *Hum. Reprod.*, **9**, 1589–1595.

Warren, J.C. and Salhanick, H.A. (1961) Steroid biosynthesis in the human ovary. *J. Clin. Endocrinol. Metab.*, **21**, 1218–30.

*Received on June 7, 1999; accepted on February 15, 2000*

The Journal of Toxicological Sciences,
Vol.27, No.2, 87-96, 2002



# ASSESSMENT OF QUANTITATIVE DUAL-PARAMETER FLOW CYTOMETRIC ANALYSIS FOR THE EVALUATION OF TESTICULAR TOXICITY USING CYCLOPHOSPHAMIDE- AND ETHINYLESTRADIOL-TREATED RATS

Chiaki KATOH[1], Satoshi KITAJIMA[2], Yumiko SAGA[2], Jun KANNO[2], Ikuo HORII[1] and Tohru INOUE[2]

[1]*Department of Preclinical Science, Nippon Roche K. K., Research Center, 200 Kajiwara, Kamakura, Kanagawa 247-8530, Japan*

[2]*Cellular and Molecular Toxicology Division, Biological Safety Research Center, National Institute of Health Science, 1-18-1 Kamiyoga, Setagaya-ku, Tokyo-158-8501, Japan*

(Received November 9, 2001; Accepted January 17, 2002)

**ABSTRACT** — In the drug discovery process, effects to the human spermatogenesis must be fully evaluated before the first human trial. To estimate testicular toxicity, histopathological evaluation has been recommended in addition to the traditional mating procedure. However, it is laborious and time-consuming. Flow cytometric analysis (FCM) has also been applied to estimate testicular toxicity because of its speed, simplicity, and the objectivity of the data. Using cyclophosphamide (CP)- and ethinylestradiol (EE)-treated rat testis, we attempted to validate our dual-parameter, DNA ploidy and cell-size FCM, in a high-throughput toxicity study. Our results showed that CP damaged some spermatogonia and some early meiotic spermatocytes and EE caused severe decrease of spermatogenic cells except for spermatogonia as well as marked decrease of somatic cells, most probably Leydig cells. This is the first report discriminating between the changes of spermatogonia and that of somatic cells with FCM analysis. These results demonstrate that this method is a very useful and powerful tool to assess testicular toxicity, especially in high-throughput toxicological studies.

**KEY WORDS:** Flow cytometry, Testis, Toxicity, Rat, Cyclophosphamide, Ethinylestradiol

## INTRODUCTION

Estimation of male infertility is a critical point for going into the first human trial of new drugs using healthy male volunteers. In addition, earlier assessment of male fertility in the drug discovery phase is a new trend in selecting clinical candidate compounds. Since testicular toxicity is an important factor for assessing fertility, a quick and fully accurate evaluation system of testicular toxicity is needed for assessment of the safety of new candidate compounds. In the traditional procedure, male reproductive toxicity has been evaluated by confirming the ability of fertility with a segment I mating procedure. As it has been generally accepted that histopathological evaluation is much more sensitive and more reliable than that of the classic reproductive study, histopathological evaluation of testicular organs has been recommended in recently revised guidelines related to reproduction and fertility (Creasy, 1997). Even so, the fact that histopathological evaluation is laborious and time-consuming makes it difficult to execute a high-throughput toxicological study for numerous chemicals or candidates.

Analysis with flow cytometry (FCM) has been applied to a variety of areas including male reproductive biology because of its speed, simplicity and the objectivity of quantitative data (Spanò and Evenson, 1993). In rodents, testicular toxicity has been evaluated with FCM using many kinds of chemicals and compounds such as nitrobenzene (Iida *et al.*, 1997), vin-

Correspondence: Chiaki KATOH

blastine (Jagetia *et al.*, 1996), methoxyacetic acid (Spanò *et al.*, 1991; Krishnamurthy *et al.*, 1998; Suter *et al.*, 1998b) and 2-bromopropane (Son *et al.*, 1999). In clinical studies, FCM analysis has also been applied for the diagnosis of human male infertility and has been proven to correlate highly with the result of histopathology (Hellstrom *et al.*, 1990; Lee and Choo, 1991; Hittmair *et al.*, 1992; Hirsch *et al.*, 1993; Giwercman *et al.*, 1994; Kostakopoulos *et al*, 1997).

In FCM analysis, testicular cells are basically divided by their ploidy into spermatozoa (Sub-N), haploid (N), diploid (2N) and tetraploid (4N). It is difficult to detect the damage of spermatogonia (2N) with ordinary DNA-FCM because too many somatic cells (Sertoli cells, Leydig cells, fibroblasts and so on) are also included in the 2N subpopulation (Hacker-Klom *et al.*, 1986; Toppari *et al.*, 1990). Thus, sensitivity is the major limitation of the FCM analysis in evaluating testicular toxicity. Several improved methods have been reported using in combination another parameter such as the somatic-specific antibody (Hittmair *et al.*, 1994), the amount of mitochondria (Petit *et al.*, 1995), or both of them (Suter *et al.*, 1997a, 1997b, 1998a, and 1998b).

In this study, we attempted to validate another approach with which testicular cells are divided by their ploidy and by cell-size. In this procedure each subpopulation of N, 2N, and 4N is further divided into two by size. The aim of this study is to assess the sensitivity and specificity of this dual-parameter FCM analysis by using a rat model treated with cyclophosphamide (CP) or ethinylestradiol (EE), both of which induce testicular toxicity but with different mechanisms. CP directly kills spermatogonia mainly by causing DNA damage, whereas EE indirectly affects the meiotic cells and post-meiotic cells by disrupting the hormonal balance (Takahashi and Matsui, 1993).

## MATERIALS AND METHODS

### Animals and test articles

CP (purity; over 97%) and EE (purity; over 98%) were purchased from Wako Pure Chemicals Industries, Ltd. (Osaka, Japan).

Male Sprague-Dawley rats (Crj: CD) were obtained from Charles River Ltd., Japan. They were individually housed in metal cages in a room with temperature of 22±2°C, relative humidity of 55±10%, and in a 12-hr light/dark cycle. A standard diet (CRF-1, Charles River Japan Ltd.) and sterilized water were given *ad libitum*.

### Experimental design

CP was dissolved with physiological saline and administered orally to 9-week-old male rats at a dose of 20 mg/kg once daily for 2 weeks. To confirm whether we could detect the decrease of other cells (theoretically pachytene spermatocytes) specifically, we set a 2-week recovery period.

On the other hand, EE was suspended in 0.5% sodium carboxymethylcellulose (CMC) solution and administered orally to 9-week-old male rats at dosages of 3 and 10 mg/kg once daily for 4 weeks. Control animals were set in each experiment and treated with each vehicle. The treated groups consisted of 5 rats each. Administration volume was 0.4 ml/100 g body weight for CP, and 0.5 ml/100 g body weight for EE. Body weights were measured twice a week. At approximately 24 hr after the final dosing, reproductive organs were excised from each animal and weighed.

The experimental designs were based on the literature (Higuchi *et al.*, 1995; Iwase *et al.*, 1995) in order to compare histopathological data and thus validate our FCM analysis.

### Isolation and staining of cells for FCM

Testicular cell suspensions were prepared according to the following method. In brief, the tunica albuginea was removed from the left testis of each animal. After treating with 0.25% Collagenase (Wako Pure Chemical Industries, Ltd., Japan) solution in Dulbecco's phosphate-buffered saline (PBS) (Dainippon Pharmaceutical Co. Ltd., Japan) at 32.5°C for about 30 min while shaking, single cell suspensions were obtained through pipetting and filtration with 40 $\mu$m and 70 $\mu$m nylon mesh (Falcon). After fixing with chilly 70% methanol, the cells were treated with 0.25% RNase (Sigma) (37°C, 20 min) followed by DNA staining with propidium iodide (PI) (Sigma).

### FCM analysis

To classify the testicular cells, the intensity of both the fluorescence and forward-scattered light (FSC) emitted from the individual cell, which show DNA content and cell size, respectively, were measured with FACSCalibur flow cytometer (Becton Dickinson, San Jose, CA). Excitation was at 488 nm with 15 mW argon-ion laser and emission at 585 nm to monitor the red fluorescence of PI. One hundred thousand cells from each sample were analyzed and relative ratios of the seven subpopulations (Sub-N, N-L, N-R, 2N-L, 2N-R, 4N-L and 4N-R; L and R represent left and right on the location of the contour plot) were determined.

The absolute count of cells was measured using the procedure described by Takizawa *et al.* (1995) based on Toppari *et al.* (1986). A constant volume of Immuno-check (standard fluorescent beads solution, EPICS, Hialeah, Florida) was added to each sample as an internal volume standard. One hundred thousand cells and beads were counted and then the total number of cells per testis was calculated from the ratio of cells to Immuno-check beads.

**Statistical analysis**

Body and organ weight data and the quantification of the identified cell subpopulations obtained from FCM were analyzed by Pitman test with $p<0.05$ and 0.01 (Pitman, 1949).

## RESULTS

**Body and reproductive organ weights**

There was no mortality in any of the groups.

Body and testicular organ weight data are shown in Table 1 and Table 2, respectively. Significant suppression of body weight gain was observed throughout the experimental period in CP- and EE-treated groups compared with the control group in each experiment. Testis weights were significantly decreased in the EE-treated groups at the dosages of 3 and 10 mg/kg. In the 20 mg/kg CP-treated group, the tendency of a decrease in the testis weight was observed but the change was not significant at both cases of 2-week administration and 2-week withdrawal. In the weights of other sexual organs (epididymides, prostate, and seminal vesicle), no changes were observed for CP but all of them were decreased for EE (data was not shown).

**FCM analysis**

On the basis of DNA content, testicular cells from mature control rats were divided into four main peaks, Sub-N (hypo-haploid cells), N (haploid cells), 2N (diploid cells) and 4N (tetraploid cells). Two distinct peaks of elongated and elongating spermatids

**Table 1.** Body weights in rats administered CP or EE.

| Cyclophosphamide (CP) | | | | |
|---|---|---|---|---|
| Dose (mg/kg) | 0 | 20 | 0 | 20 |
| | 2-week administration | | 2-week recovery | |
| Number of rats | 5 | 4 | 5 | 5 |
| Days of treatment | | | | |
| 0 | 322.8 ± 9.4 | 330.0 ± 8.0 | 391.2 ± 19.6 | 333.4 ± 19.6** |
| 3 | 339.2 ± 11.6 | 334.5 ± 7.7 | 393.6 ± 24.2 | 339.0 ± 13.4** |
| 7 | 359.6 ± 16.6 | 334.3 ± 27.0 | 412.0 ± 26.4 | 358.8 ± 12.0** |
| 10 | 376.0 ± 17.8 | 339.5 ± 21.7* | 430.4 ± 30.8 | 378.2 ± 13.8** |
| 14 | 393.8 ± 21.8 | 338.8 ± 29.7* | 442.0 ± 29.0 | 383.6 ± 11.7** |

| Ethinylestradiol (EE) | | | |
|---|---|---|---|
| Dose (mg/kg) | 0 | 3 | 10 |
| Number of rats | 5 | 5 | 5 |
| Days of treatment | | | |
| 0 | 372.0 ± 8.8 | 373.6 ± 10.9 | 373.2 ± 5.9 |
| 3 | 383.4 ± 11.0 | 362.8 ± 12.3* | 356.0 ± 8.0** |
| 7 | 391.2 ± 15.0 | 329.8 ± 20.9** | 320.4 ± 6.8** |
| 10 | 407.6 ± 20.2 | 330.8 ± 23.0** | 322.2 ± 7.9** |
| 14 | 423.8 ± 26.8 | 327.4 ± 22.7** | 308.4 ± 4.5** |
| 17 | 438.4 ± 26.8 | 326.0 ± 24.5** | 300.0 ± 3.7** |
| 21 | 450.4 ± 32.7 | 329.6 ± 23.8** | 298.0 ± 10.7** |
| 24 | 459.0 ± 34.8 | 331.0 ± 20.6** | 298.4 ± 12.5** |
| 28 | 467.4 ± 34.8 | 328.0 ± 19.5** | 297.0 ± 9.7** |

*, **: Significantly different from control group ($p<0.05$, $p<0.01$).

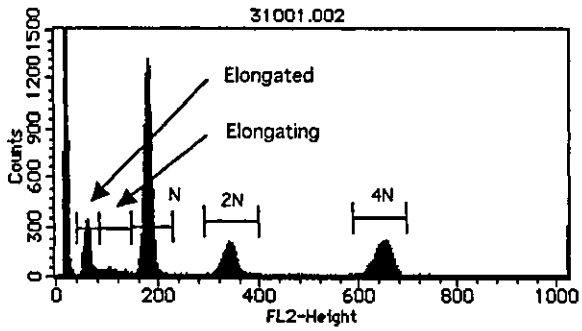


**Fig. 1.** Representative single parameter DNA-fluorescence distribution after staining with PI.
Histogram shows testicular cell subpopulations from a control rat. Elongating and elongated spermatids (sub-N), round spermatids (N), diploid cells (2N), and tetraploid cells (4N) are discernible according to their DNA ploidy.

were observed in the Sub-N population (Fig. 1). The application of another parameter, cell size, enables us to further divide by two the N, 2N and 4N subpopulations, so that the testicular cells could be classified into a total of seven subpopulations in the normal control rat (Fig. 2). With the FACS cell-sorting analysis, the distribution of each kind of testicular cell could be confirmed by its morphological aspects (our preliminary data). Sub-N subpopulation included elongated and some elongating spermatids. Round and all the rest of elongating spermatids were divided into two subpopulations by their cell sizes, N-L (smaller and probably differentially more advanced) and N-R (larger). Whereas the 2N-R subpopulation mainly included larger somatic cells (Sertoli cells, Leydig cells), 2N-L contained smaller somatic cells (peritubular myoid cells and fibroblasts, etc.) and germ cells (resting or G1/G2 phase spermatogonia and secondary spermatocytes). Smaller spermatocytes (mainly leptotene and zygotene phases) were located in 4N-L and larger spermatocytes (mainly pachytene and diplotene phases) in 4N-R. Both the relative percentages and the absolute counts of testicular cells in each subpopulation were calculated for each animal.

**Cytotoxic effects of compounds on different spermatogenic cells**

Cyclophosphamide (CP). CP was administered to 9-week-old rats for 2 weeks at a dosage level of 20 mg/kg. Fig. 3A shows the result with a single-parameter, DNA-FCM as the ordinal method. With the DNA-FCM analysis, we could not detect any changes in any subpopulation at the end of the 2-week administration period. On the other hand, the dual-parameter FCM analysis showed a significant decrease of both the relative percentages and the absolute counts of 2N-L and 4N-L (Fig. 3B, C). In addition, 2N-R showed a significant increase in the relative percentage but not the absolute count, which indicated that the decrease of 2N-L and 4N-L cells resulted in an increased relative ratio of 2N-R. These results indicated that spermatogonia and early meiotic cells were affected with 2-week

**Table 2.** Testicular organ weights in rats administered CP or EE.

| Cyclophosphamide (CP) | | | | |
|---|---|---|---|---|
| Dose (mg/kg) | 0 | 20 | 0 | 20 |
| | 2-week administration | | 2-week recovery | |
| Number of rats | 5 | 4 | 5 | 5 |
| Organ Weight (mg) | | | | |
| Testis-R | 1701.0 ± 80.9 | 1525.6 ± 140.8 | 1608.5 ± 99.1 | 1586.6 ± 173.3 |
| Testis-L | 1690.6 ± 78.8 | 1537.7 ± 138.6 | 1652.2 ± 96.0 | 1588.8 ± 155.4 |

| Ethinylestradiol (EE) | | | |
|---|---|---|---|
| Dose (mg/kg) | 0 | 3 | 10 |
| Number of rats | 5 | 5 | 5 |
| Organ Weight (mg) | | | |
| Testis-R | 1691.2 ± 133.8 | 627.2 ± 159.4** | 473.0 ± 92.3** |
| Testis-L | 1709.0 ± 133.2 | 609.6 ± 169.1** | 478.8 ± 118.4** |

*, **: Significantly different from control group ($p<0.05$, $p<0.01$).

CP treatment. In the 2-week recovery test, a significant decrease of 4N-R in both the relative percentage and the absolute count were detected (Fig. 4B, C). The increase of N-L was observed significantly for the relative ratio but not for the absolute count. The DNA-FCM also detected a significant decrease of 4N after 2-week withdrawal (Fig. 4A). Thus, the DNA-FCM could be used for detecting severe or moderate changes but not slight changes such as 2N-L and 4N-L from CP-treated rats for 2 weeks. These results indicate that our dual-parameter FCM was more sensitive and more informative in evaluating the cytotoxic changes in spermatogenesis than the traditional single-parameter, DNA-FCM.

Ethinylestradiol (EE). 9-week-old rats were treated with EE at dosages of 0, 3, and 10 mg/kg for 4 weeks. With the DNA-FCM (Fig. 5A), a significant decrease of spermatids (elongated, elongating and round) and significant increase of 2N were observed. No change was observed for 4N, which indicated that 4N was also affected. The results of dual-parameter FCM analysis are shown in Fig. 5B, C. For the relative ratio of cells, a significant decrease of Sub-N, N-L and 4N-R and a significant increase of 2N-L and 4N-L were observed in the 3 and 10 mg/kg dosing groups. Furthermore, the relative ratio of 2N-R cells was significantly decreased at 10 mg/kg. For the absolute counts, cells in all subpopulations besides 2N-L were shown to be markedly depleted in a dose-dependent manner. Thus, a significant decrease of N-R at both dosages and 2N-R at 3 mg/kg could be detected for the

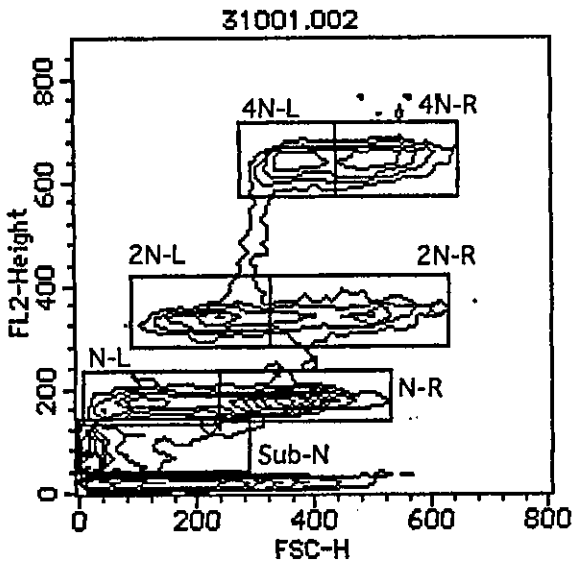


**Fig. 2.** Contour density plot representation of DNA ploidy vs. cell size of testicular cells from a control rat. With their ploidy, testicular cells are divided into four major peaks (sub-N, N, 2N and 4N) (Fig. 1). N, 2N, and 4N subpopulations were further divided into two by size, discriminated as -L and -R. As a result, total 7 subpopulations are classified with our dual-parameter FCM.

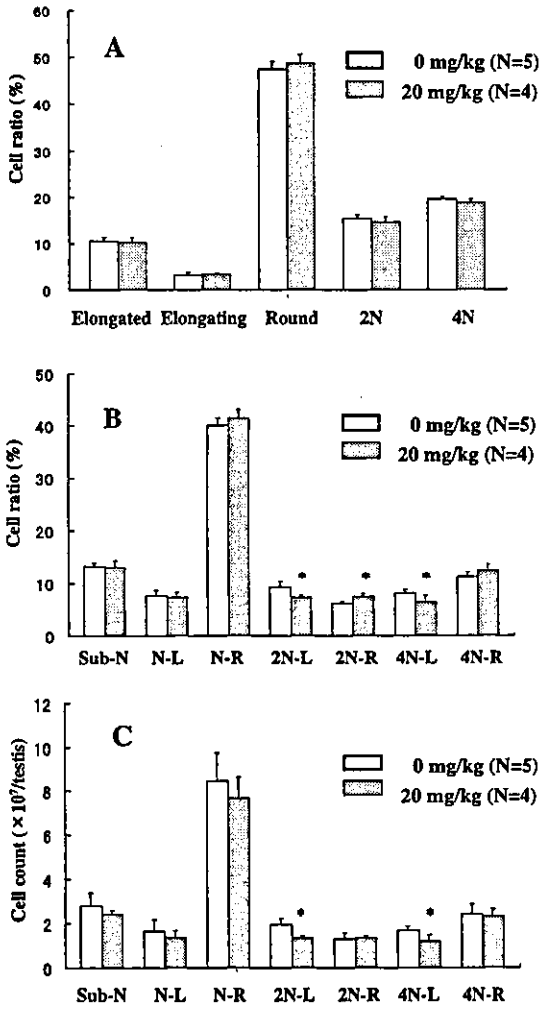


**Fig. 3.** The effects of testicular cells in each subpopulation 2 weeks after cyclophosphamide (20 mg/kg, p.o.) treatment.
(A) relative cell ratios with single-parameter, DNA-FCM.
(B) relative cell ratios with dual-parameter FCM.
(C) absolute cell counts with dual-parameter FCM.
*, **: Significantly different from control group ($p<0.05$, $p<0.01$).

absolute counts but not for the relative ratios. Other discrepancies between the relative cell ratios and the absolute counts were seen with 2N-L and 4N-L. As for the relative ratio, both 2N-L and 4N-L significantly increased, but for the absolute counts no change or significant decrease was seen, respectively. These results revealed that the increased ratios of 2N-L and 4N-L were due to the marked depletion of cells in other subpopulations. In addition, the results obtained from absolute counts indicated that after 4 weeks of EE treatment, most spermatogonia remained, but other testicular cells including somatic cells (most likely Leydig cells) exhibited cytotoxic changes.

## DISCUSSION

Compared with histopathological examination, although DNA-FCM can't detect quantitative changes

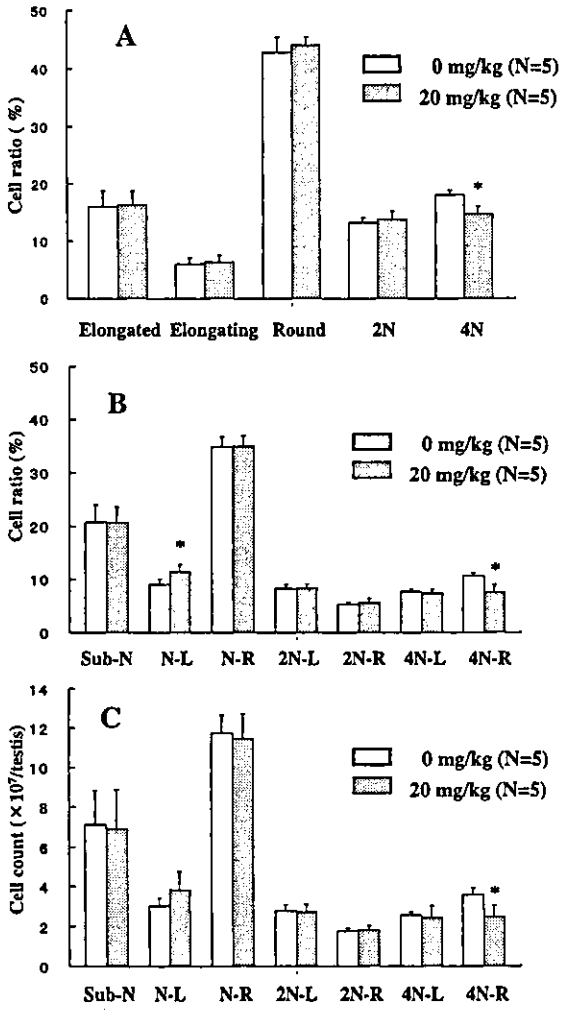


Fig. 4. The effects of testicular cells in each subpopulation 2 weeks after cyclophosphamide (20 mg/kg, p.o.) withdrawal.
(A) relative cell ratios with single-parameter, DNA-FCM.
(B) relative cell ratios with dual-parameter FCM.
(C) absolute cell counts with dual-parameter FCM.
*, **: Significantly different from control group ($p<0.05$, $p<0.01$).

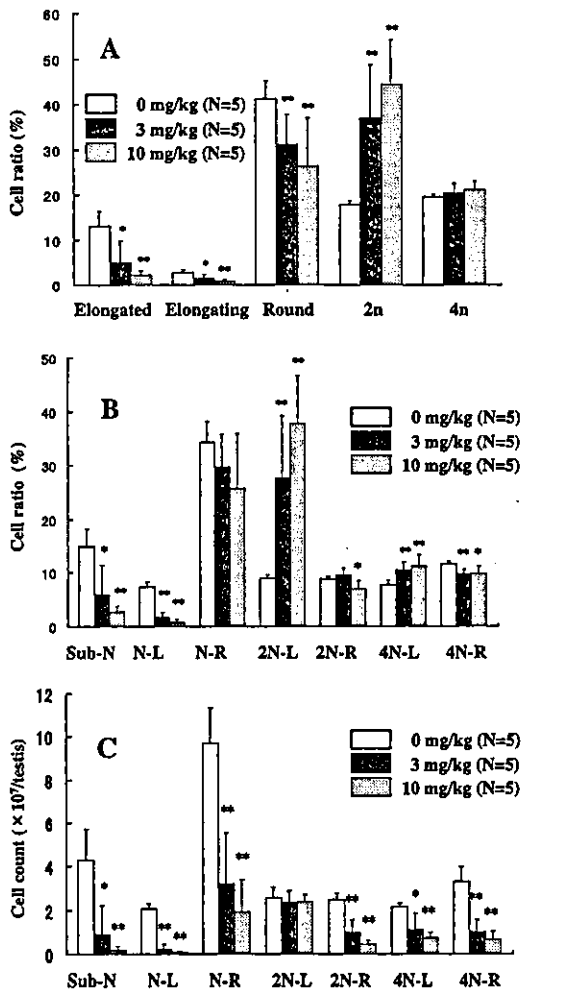


Fig. 5. The effects of testicular cells in each subpopulation 4 weeks after ethinylestradiol (10, 30 mg/kg, p.o.) treatment.
(A) relative cell ratios with single-parameter, DNA-FCM.
(B) relative cell ratios with dual-parameter FCM.
(C) absolute cell counts with dual-parameter FCM.
*, **: Significantly different from control group ($p<0.05$, $p<0.01$).

(vacuolation of Sertoli cells etc.), procedures of FCM lead to apply a high-throughput approach in terms of speed, objectivity, and no limitation of counts. We applied an improved method that classifies testicular cells into 7 subpopulations by both ploidy and size. Four peaks of testicular cells are discernible by their ploidy, namely Sub-N, N, 2N, and 4N, in rats. Because of the reduced binding of propidium iodide accompanied with DNA compaction, the peak of Sub-N can be distinguished from that of N (Spanò and Evenson, 1993). 2N and 4N as well as N could be further divided into -L (smaller) and -R (larger) by cell size. Cell size not only relates to the stage of differentiation, but also might enable separation of somatic cells from germ cells in the 2N subpopulation. Therefore, we considered that a dual-parameter FCM might be superior to the traditional DNA-FCM analysis. In this study we assessed the sensitivity and specificity of this dual-parameter FCM by using rats treated with CP and EE as well-known testicular toxicants.

CP belongs to the class of oxazaphosphorines, and the bioactivated metabolites are alkylating agents that show cytostatic effects by forming covalent DNA adducts. The cells most affected by CP are spermatogonia, although leptotene spermatocytes are also partly damaged (Matsui *et al.*, 1995). It is reported that detection of a decrease in spermatogenic cells caused by CP is difficult even with histopathological analysis without quantitative morphometric evaluation (Takahashi and Matsui, 1993; Matsui *et al.*, 1995).

In our study, after dosing at 20 mg/kg CP for 2 weeks, a tendency of decrease in testis weight was observed but was not significant. Neither was an obvious change observed by the traditional classification using the single parameter of DNA ploidy in FCM analysis. In contrast, a significant decrease was observed in 2N-L and 4N-L with our dual-parameter FCM based on the ploidy and cell size, suggesting that spermatogonia and early meiotic cells were affected. These dual-parameter results well-matched the histopathological data by Higuchi *et al.* (1995), Kaneto *et al.* (1999a), Watanabe *et al.* (2000) and Matsumoto *et al.* (2000). They reported that dosing at 20 mg/kg of CP for 2 weeks resulted in a decrease of spermatogonia, preleptotene spermatocytes and zygotene spermatocytes. After a 2-week recovery period, a decrease of 4N was observed with the DNA-FCM. Furthermore, the dual-parameter FCM showed a decrease of only 4N-R, indicating that the damage shifted to late meiotic spermatocytes during 2 weeks and was not inconsistent with the course of the spermatogenic differentiation cycle. Thus, applying the dual-parameter FCM but not the single-parameter, DNA-FCM, we could detect the decrease of spermatogonia and also discriminate between the change of early spermatocytes and that of late spermatocytes. These results demonstrate that the dual-parameter FCM has much higher sensitivity than the traditional DNA-FCM.

To investigate another pattern of spermatogenic failure, EE was given to rats for 4 weeks at dosages of 3 and 10 mg/kg. The data of relative ratios showed significant decreases of Sub-N, N-L, and 4N-R and significant increases of 2N-L and 4N-L in both of the treated groups. 2N-R was also significantly decreased at 10 mg/kg. On the other hand, the data of absolute counts showed a marked depletion of all subpopulations other than 2N-L in a dose-dependent manner, even though a slight decrease of 2N-L was also observed in a few animals. These discrepancies between the results from relative ratios and absolute counts demonstrate that the evaluation with absolute counts is essential in precisely assessing the cytotoxic changes in cases in which more than two different kinds of cells are affected simultaneously. The results from our FCM analysis are in accordance with the histopathological evaluation by Iwase *et al.* (1995), Kaneto *et al.* (1999b) Miyamoto *et al.* (2000) and Kinomoto *et al.* (2000). Kaneto *et al.* (1999b) showed that dosages of 10 mg/kg EE resulted in a decrease of spermatocytes primarily, but spermatogonia was well-preserved for 2 weeks. However, after 3 weeks of dosing, quantitative morphometric evaluation was reported to be impossible due to severe atrophic changes in almost all tubules. Our overall counting of cells in a testis with FCM could reveal that spermatogonia was still well-preserved after 4 weeks of dosing compared with other spermatogenic cells. Determining whether spermatogonia is affected or not is a critical point to assess testicular toxicity. FCM could be helpful for evaluating the target cells or action mechanisms even in these severe conditions. Furthermore, one dispute in morphometric analysis is whether counting the frequency of stages in seminiferous tubules is needed to detect the delay of spermatogenesis (Creasy, 1997). The ability to quantify the overall changes is the benefit of the FCM analysis. In addition, it should be emphasized that we can definitely discriminate between the decrease of Leydig cells with EE and the decrease of spermatogonia with CP in the 2N subpopulation. This is the first report on a definitive detection of the decrease of somatic cells (Leydig cells) in the FCM analysis.

Recently, new approaches for detecting testicular toxicity with FCM have been reported; for example, detection of apoptosis (Krishnamurthy *et al.*, 1998; Shiratsuchi *et al.*, 1997), delay of spermatogenesis with BrdU staining (Weinbauer *et al.*, 1998) and precise classification with the combination of other parameters (Suter *et al.*, 1997b, 1998a and 1998b). Our procedure is suitable to combine with another staining kit, especially for a specific antibody, because the membrane of isolated cells remains intact due to no use of severe treatments with trypsin, detergent or pepsin. Such research is under investigation in our laboratory.

In summary, we assessed the dual-parameter, DNA ploidy and cell size, FCM in the detection of cytotoxic changes of testicular cells after treatment with CP and EE. The overall changes of testicular cell counts causing CP and EE are summarized in Table 3. These results showed that CP mainly damaged spermatogonia and early-phase meiotic cells by 2 weeks. In contrast, spermatogonia were relatively refractory to EE, but other spermatogenic cells were severely damaged. Leydig cells were also probably reduced with EE. These indications from our dual-parameter FCM analysis corresponded well to the histopathological findings reported in recent literature. This method is a very useful and powerful tool to assess spermatogenic failures, especially in high-throughput toxicological studies, because of its simplicity, quickness, and preciseness.

This study was carried out with financial assistance from the Human Science Foundation in the Ministry of Public Welfare in Japan.

## ACKNOWLEDGMENT

The authors thank Noriko Moriyama, Biological Safety Research Center, National Institute of Health Science for expert technical assistance.

## REFERENCES

Creasy, D.M. (1997): Evaluation of testicular toxicity in safety evaluation studies: The appropriate use of spermatogenic staging. Toxicol. Pathol., **25**, 119-131.

Giwercman, A., Clausen, O.P., Bruun, E., Frimodt-Moller, C. and Skakkebaek, N.E. (1994): The value of quantitative DNA flow cytometry of testicular fine-needle aspirates in assessment of spermatogenesis: A study of 137 previously maldescended human testes. Int. J. Androl., **17**,

**Table 3.** Summary of results with FCM compared with histopathological data.

| | | | | | | | |
|---|---|---|---|---|---|---|---|
| Somatic cells; | | Sertoli, Leydig | Myoid, Fibro | | | | |
| Spermatogenic cells; | | | Gonia → L/Z → P/D | | | | |
| | | | Sp II ← ┘ | | | | |
| | | | ↓ | | | Round → | Elongating |
| Ploidy | | 2N-R | 2N-L | 4N-L | 4N-R | N-R | N-L |
| CP | FCM | → | ↓ | ↓ | → | → | → |
| (2 wk) | | | | | | | |
| | Histo | | decrease of Gonia | decrease of L/Z/early P | | | |
| (2 wk recovery) | FCM | → | → | → | ↓ | → | → |
| EE | FCM | ↓↓ | → | ↓～↓↓ | ↓↓ | ↓↓ | ↓↓ |
| (4 wk) | | | | | | | |
| | Histo | Leydig atrophy | | degeneration of Spermatocytes | | degeneration of Spermatids | |

→ No changes.

↓, ↓↓: decrease with statistical significance at $p<0.05$ and $p<0.01$ for FCM analysis.

Histopathological data was obtained from Higuchi *et al.* (1995), Kaneto *et al.* (1999a), Matsumoto *et al.* (2000) and Watanabe *et al.* (2000) for CP and Iwase *et al.* (1995), Kaneto *et al.* (1999b), Miyamoto *et al.* (2000) and Kinomoto *et al.* (2000) for EE. Only quantitative changes are shown in this table.

Abbreviations: Histo: histopathological examination, Fibro: fibroblasts, Myoid: peritubular myoid cells, Gonia: spermatogonia, SpII; secondary spermatocytes, L: leptotene, Z: zygotene, P: pachytene, D: diplotene spermatocytes, round: round spermatids, elongating: elongating spermatids

35-42.

Hacker-Klom, U.B., Meistrich, M.L. and Gohde, W. (1986): Effect of doxorubicin and 4'-epi-doxorubicin on mouse spermatogenesis. Mutat. Res., **160**, 39-46.

Hellstrom, W.J., Tesluk, H., Deitch, A.D. and de Vere White, R.W. (1990): Comparison of flow cytometry to routine testicular biopsy in male infertility. Urology, **35**, 321-326.

Higuchi, H., Nakaoka, M., Katsuda, Y., Kawamura, S., Kato, T. and Matsuo, M. (1995): Collaborative assessment of optimal administration period and parameters to detect effects on male fertility in the rat: Effects of cyclophosphamide on the male reproductive system. J.Toxicol. Sci., **20**, 239-249.

Hirsch, I.H., McCue, P., Kulp-Hugues, D., Sedor, J. and Flanigan, M. (1993): Validation of flow cytometry analysis in the objective assessment of spermatogenesis: Comparison to the quantitative testicular biopsy. J. Urol., **150**, 342-346.

Hittmair, A., Rogatsch, H., Offner, F., Feichtinger, H., Ofner, D. and Mikuz, G. (1992): Deoxyribonucleic acid flow cytometry and semiquantitative histology of spermatogenesis: A comparative study. Fertil. Steril., **58**, 1040-1045.

Hittmair, A., Rogatsch, H., Mikuz, G. and Feichtinger, H. (1994): Quantification of spermatogenesis by dual-parameter flow cytometry. Fertil. Steril., **61**, 746-750.

Iida, S., Misaka, H. and Naya, M. (1997): A flow cytometric analysis of cytotoxic effects of nitrobenzene on rat spermatogenesis. J. Toxicol. Sci., **22**, 397-407.

Iwase, T., Sano, F., Murakami, T. and Inazawa, K. (1995): Male reproductive toxicity of ethinylestradiol associated with 4 weeks daily dosing prior to mating in rats. J. Toxicol. Sci.,**20**, 265-279.

Jagetia, G.C., Krishnamurthy, H. and Jyothi, P. (1996): Evaluation of cytotoxic effects of different doses of vinblastine on mouse spermatogenesis by flow cytometry. Toxicology, **112**, 227-236.

Kaneto, M., Kanamori, S., Hara, K. and Kishi, K. (1999a): Characterization of epididymal sperm motion and its correlation with stages of target cells in rats given $\alpha$-chlorohydrin, cyclophosphamide or nitrazepam. J. Toxicol. Sci., **24**, 187-197.

Kaneto, M., Kanamori, S., Hishikawa, A. and Kishi, K. (1999b): Epididymal sperm motion as a parameter of male reproductive toxicity: Sperm motion, fertility, and histopathology in ethinylestradiol-treated rats. Reprod. Toxicol., **13**, 279-289.

Kinomoto, T., Sawada, M., Ogawa, S., Iguchi, A., Matsui, A., Iino, Y., Shiraishi, Y., Nishi, N. and Mera, Y. (2000): Collaborative work to evaluate toxicity on male reproductive organs by repeated dose studies in rats 3). Effects of repeated doses of ethinylestradiol for 2 and 4 weeks on the male reproductive organs. J. Toxicol. Sci., **25**, Special issue, 43-49.

Kostakopoulos, A., Georgoulakis, J., Deliveliotis, Ch., Spanakis, G., Filippidou, A. and Tamvakis, N. (1997): Deoxyribonucleic acid flow cytometry in the assessment of spermatogenesis. J. Urol., **158**, 79-81.

Krishnamurthy, H., Weinbauer, G.F., Aslam, H., Yeung, C.H. and Nieschlag, E. (1998): Quantification of apoptotic testicular germ cells in normal and methoxyacetic acid-treated mice as determined by flow cytometry. J. Androl., **19**, 710-717.

Lee, S.E. and Choo, M.S. (1991): Flow-cytometric analysis of testes in infertile men: A comparison of the ploidy to routine histopathologic study. Eur. Urol., **20**, 33-38.

Matsui, H., Mitsumori, K., Yasuhara, K., Onodera, H., Shimo, T. and Takahashi, M. (1995): Morphological evaluation of cyclophosphamide testicular toxicity in rats using quantitative morphometry of spermatogenic cycle stages. J. Toxicol. Sci., **20**, 407-414.

Matsumoto, S., Hirakawa, M., Shimomoto, T., Sato, M., Kitaura, K. and Minami, T. (2000): Collaborative work to evaluate toxicity on male reproductive organs by repeated dose studies in rats 13). Effects of a single oral dose of cyclophosphamide. J. Toxicol. Sci., **25**, Special issue, 139-143.

Miyamoto, Y., Ueda, K., Oshida, K. and Ohmori, E. (2000): Collaborative work to evaluate toxicity on male reproductive organs by repeated dose studies in rats 2). Testicular toxicity in rats treated orally with ethinylestradiol for 2 weeks. J. Toxicol. Sci., **25**, Special issue, 33-42.

Petit, J.M., Ratinaud, M.H., Cordelli, E., Spanò M. and Julien, R. (1995): Mouse testis cell sorting according to DNA and mitochondrial changes during spermatogenesis. Cytometry, **19**, 304-312.

Pitman, E.J.G. (1949): Lecture Notes on Nonparametric Statistical Inference, Columbia Univ.

Shiratsuchi, A., Umeda, M., Ohba, Y. and Nakanishi, Y. (1997): Recognition of phosphatidylserine on the surface of apoptotic spermatogenic cells and subsequent phagocytosis by Sertoli cells of the rat. J. Biol. Chem., **272**, 2354-2358.

Son, H.Y., Kim, Y.B., Kang, B.H., Cho, S.W., Ha, C.S. and Roh, J.K. (1999): Effects of 2-bromopropane on spermatogenesis in the Sprague-Dawley rat. Reprod. Toxicol., **13**, 179-187.

Spanò, M., Amendola, R., Bartoleschi, C., Emiliani, S., Cordelli, E., Petit, J.M., Julien, R. and Ratinaud, M.H. (1991): Evaluation of 2-methoxyacetic acid toxicity on mouse germ cells by flow cytometry. J. Toxicol. Environ. Health., **34**, 157-176.

Spanò, M. and Evenson, D.P. (1993): Flow cytometric analysis for reproductive biology. Biol. Cell, **78**, 53-62.

Suter, L., Koch, E., Bechter, R. and Bobadilla, M. (1997a): Three-parameter flow cytometric analysis of rat spermatogenesis. Cytometry, **27**, 161-168.

Suter, L., Bobadilla, M., Koch, E. and Bechter, R. (1997b): Flow cytometric evaluation of the effects doxorubicin on rat spermatogenesis. Reprod. Toxicol., **11**, 521-531.

Suter, L., Clemann, N., Koch, E., Bobadilla, M. and Bechter, R. (1998a): New and traditional approaches for the assessment of testicular toxicity. Reprod. Toxicol., **12**, 39-47.

Suter, L., Meier, G., Bechter, R. and Bobadilla, M. (1998b): Flow cytometry as a sensitive tool to assess testicular damage in rat. Arch. Toxicol., **72**, 791-797.

Takahashi, M. and Matsui, H. (1993): Mechanisms of testicular toxicity. J. Toxicol. Pathol., **6**, 161-174.

Takizawa, S., Katoh, C., Fukatsu, N. and Horii, I. (1995): Flow cytometric analysis for the evaluation of the rat sperm viability and number in the male reproductive toxicity studies. Cong. Anom., **35**, 177-187.

Toppari, J., Mali, P. and Eerola, E. (1986): Rat spermatogenesis *in vitro* traced by quantitative flow cytometry. J. Histochem. Cytochem., **34**, 1029-1035.

Toppari, J., Bishop, P.C., Parker, J.W., Ahmad, N., Girgis, W. and diZerega, G.S. (1990): Cytotoxic effects of cyclophosphamide in the mouse seminiferous epithelium: DNA flow cytometric and morphometric analysis. Fundam. Appl. Toxicol., **15**, 44-52.

Watanabe, T., Yamaguchi, N., Akiba, T., Tanaka, M. and Takimoto, M. (2000): Collaborative work to evaluate toxicity on male reproductive organs by repeated dose studies in rats 12) effects of cyclophosphamide on spermatogenesis. J. Toxicol. Sci., **25**, Special issue, 129-137.

Weinbauer, G.F., Schubert, J., Yeung, C.H., Rosiepen, G. and Nieschlag, E. (1998): Gonadotrophin-releasing hormone antagonist arrests premeiotic germ cell proliferation but does not inhibit meiosis in the male monkey: A quantitative analysis using 5-bromodeoxyuridine and dual parameter flow cytometry, J. Endocrinol., **156**, 23-34.

0013-7227/03/$15.00/0
Printed in U.S.A.

Endocrinology 144(6):2597–2605

doi: 10.1210/en.2002-220980

# Expression of a Novel C-Type Lectin in the Mouse Vagina

YOSHINAO KATSU, DENNIS B. LUBAHN, AND TAISEN IGUCHI

*Center for Integrative Bioscience, Okazaki National Research Institutes (Y.K., T.I.), Okazaki 444-8585, Japan; Core Research for Evolutional Science and Technology of Japan, Science and Technology Corporation (Y.K., T.I.); Department of Molecular Biology, University of Missouri (D.B.L.), Columbia, Missouri 65211; and Department of Molecular Biomechanics, School of Life Science, Graduate University of Advanced Studies (T.I.), Okazaki 444-8585, Japan*

**Estrogens regulate the proliferation and differentiation of mouse vaginal epithelial cells. However, the molecular mechanisms underlying estrogen-induced changes have not been elucidated. The goal of this study was to identify estrogen-responsive genes related to the proliferation and differentiation of mouse vaginal epithelial cells. We used differential display to reveal specific genes regulated by estrogens and identified a transcript that was designated DDV10. DDV10 encodes a membrane protein with a C-type lectin domain in the carboxyl-terminal region; thus, we inferred that it belongs to the C-type lectin family. We analyzed the temporal and spatial expression of DDV10 using RT-PCR, quantitative real-time RT-PCR, and *in situ* hybridization. Ovariectomy decreased DDV10 mRNA levels, whereas 17β-estradiol treatment increased expression of DDV10 mRNA in vaginas of ovariectomized mice. DDV10 mRNA was first detected between 20 and 30 d after birth and was found in eye, tongue, stomach, and stratified and cornified vaginal epithelial cells, but not in stromal cells or uterus. DDV10 transcripts were not detected in vaginas of estrogen receptor α knockout mice. Taken together, these data suggest that DDV10 encodes a novel, 17β-estradiol-regulated, C-type lectin in the mouse vagina. DDV10 may play a role in the stratification and/or cornification of epithelial cells during differentiation. (*Endocrinology* 144: 2597–2605, 2003)**

PROLIFERATION and differentiation of the vaginal epithelium are regulated by the natural hormone, 17β-estradiol (E2), which modifies cellular physiology by modulating the transcriptional activity of specific nuclear estrogen receptors (ERs). Estrogens are believed to stimulate primary response genes, initiating a cascade of transcriptional events, the products of which participate in physiological responses known to be estrogen-dependent events in the target organs *in vivo*. The multifaceted role of estrogens within the female reproductive tract has been well studied and characterized. However, the regulation of vaginal gene expression by estrogens and the molecular mechanisms underlying estrogen-mediated proliferation remain unclear.

In addition to stimulating vaginal epithelial proliferation, estrogens elicit a complex pattern of differentiative events in vaginal epithelium. The rodent vaginal epithelium exhibits cyclical changes in response to cyclical ovarian secretions, displaying an alternating pattern of keratinization and mucification (1). The vaginal epithelium of the ovariectomized mouse is atrophied to two or three cell layers. In response to estrogens, basal epithelial cells proliferate rapidly, leading to the formation of a highly stratified epithelium. The postmitotic suprabasal cells differentiate as they move outward through the epithelium, becoming enlarged and undergoing structural and morphological changes indicative of cornification. The apical layer becomes heavily keratinized. These morphological changes, in response to estrogens, are accompanied by the production of cytokeratins 1 and 10, markers common to epidermal and vaginal epithelial differentiation (2).

Singh and Gupta (3) showed that treatment with estrogens induces a change in intracellular calcium levels, and calcium is essential for normal epidermal differentiation (4). It is known that normal epidermal cells (keratinocytes) form cornified envelopes in response to calcium as a result of cross-linking of substrates such as involucrin by a specific membrane-bound enzyme, transglutaminase-1 (5, 6). However, the molecular mechanisms underlying calcium-inducible differentiation of keratinocytes is unclear beyond the potential involvement of protein kinase C and/or calcium receptor (7, 8).

E2 stimulates epithelial cell proliferation in the female genital tract indirectly through stromal ERα via a paracrine mechanisms. Our objective in this study was to analyze the mechanism of E2-induced proliferation and differentiation of the vaginal epithelium. Using differential display/RT-PCR, we isolated a new member of the C-type lectin family that is expressed in vagina with proliferating and cornified epithelium. Characterization of mRNA expression indicates that estrogen regulates the gene encoding this novel C-type lectin in mouse vagina. Furthermore, this C-type lectin is found in epithelial cells, but not in stromal cells, suggesting that it may be an important factor in the stratification and/or cornification of the vaginal epithelium of mice.

Abbreviations: $C_T$, Threshold cycle; DD/RT-PCR, differential display/RT-PCR; DES, diethylstilbestrol; E2, 17β-estradiol; ER, estrogen receptor; ERαKO, ERα knockout; GAPDH, glyceraldehyde phosphate dehydrogenase; OCIL, osteoclast inhibitory lectin; oligo(dT), oligo(deoxythymidine); OVX, ovariectomized, ovariectomy; PKC, protein kinase C; Q-PCR, quantitative PCR; SSC, standard saline citrate.

## Materials and Methods

### *RNA isolation, Northern blotting, RT-PCR, and quantitative PCR (Q-PCR)*

Total RNA was isolated using RNeasy kit (QIAGEN, Chatsworth, CA). For Northern blot analysis, 20 μg total RNA/lane were denatured